Global distribution of whistler-mode chorus waves observed on the THEMIS spacecraft

W. Li,[1] R. M. Thorne,[1] V. Angelopoulos,[2] J. Bortnik,[1] C. M. Cully,[3] B. Ni,[1] O. LeContel,[4] A. Roux,[4] U. Auster,[5] and W. Magnes[6]

Received 3 February 2009; revised 13 March 2009; accepted 23 March 2009; published 7 May 2009.

[1] Whistler mode chorus waves are receiving increased scientific attention due to their important roles in both acceleration and loss processes of radiation belt electrons. A new global survey of whistler-mode chorus waves is performed using magnetic field filter bank data from the THEMIS spacecraft with 5 probes in near-equatorial orbits. Our results confirm earlier analyses of the strong dependence of wave amplitudes on geomagnetic activity, confinement of nightside emissions to low magnetic latitudes, and extension of dayside emissions to high latitudes. An important new finding is the strong occurrence rate of chorus on the dayside at $L > 7$, where moderate dayside chorus is present >10% of the time and can persist even during periods of low geomagnetic activity.
Citation: Li, W., R. M. Thorne, V. Angelopoulos, J. Bortnik, C. M. Cully, B. Ni, O. LeContel, A. Roux, U. Auster, and W. Magnes (2009), Global distribution of whistler-mode chorus waves observed on the THEMIS spacecraft, *Geophys. Res. Lett.*, *36*, L09104, doi:10.1029/2009GL037595.

1. Introduction

[2] Chorus waves are intense whistler mode electromagnetic emissions characterized by a sequence of discrete elements typically in the range of 0.1–0.8 f_{ce} [*Santolik et al.*, 2003]. Chorus emissions are often observed in two bands, with a gap at 0.5 f_{ce} [e.g., *Tsurutani and Smith*, 1974], and both upper-band and lower-band chorus are dependent on geomagnetic activity [e.g., *Tsurutani and Smith*, 1974; *Meredith et al.*, 2001, 2003]. The generation region of chorus is located outside the plasmapause near the geomagnetic equator [*LeDocq et al.*, 1998; *Santolík et al.*, 2003] and chorus waves are associated with enhanced fluxes of suprathermal electrons injected from the plasma sheet [e.g., *Anderson and Maeda*, 1977; *Li et al.*, 2008, 2009]. Recently, whistler-mode chorus waves have received increased attention due to their important roles in both acceleration and loss of energetic radiation belt electrons [e.g., *Horne and Thorne*, 1998, 2003; *Summers et al.*, 1998, 2002, 2007; *Lorentzen et al.*, 2001; *Meredith et al.*, 2002, 2003; *O'Brien et al.*, 2004; *Horne et al.*, 2005; *Shprits et al.*, 2006; *Thorne et al.*, 2005, 2007; *Li et al.*, 2007], but better information is required on the global distribution of chorus waves.

[3] Previous statistical analyses [e.g., *Tsurutani and Smith*, 1977; *Parrot and Gaye*, 1994; *Meredith et al.*, 2003; *Santolik et al.*, 2005] captured important features of the global distribution of chorus waves, showing that chorus activity is dependent on geomagnetic activity and occurs over a wide range of geospace. Their analyses also demonstrated that intense nightside chorus is confined near the magnetic equator (<15°), while strong dayside chorus can extend to higher magnetic latitudes (>15°). However, the data coverage was still limited with previous spacecraft only (e.g., CRRES is largely confined within 7 R_e with a pronounced data gap in the pre-noon sector for $L > 5$).

[4] Data from the THEMIS spacecraft are used here to examine the global distribution of the chorus magnetic field intensities as a function of magnetic activity, as well as its occurrence rate, to identify where these chorus waves should be most effective to cause acceleration or precipitation of energetic electrons. This analysis not only provides complementary information to the earlier statistical analyses but also points out new important characteristics on the global distribution of chorus waves.

2. THEMIS Data Analysis

[5] The THEMIS spacecraft, comprising 5 probes in the near-equatorial orbits with apogees above 10 R_e and perigees below 2 R_e [*Angelopoulos*, 2008], are ideally situated to measure the chorus emissions in the equatorial magnetosphere. The Digital Fields Board (DFB) [*Cully et al.*, 2008a] calculates the mean amplitude of the electric and magnetic fields in 6 logarithmically-spaced frequency bands from 0.1 Hz to 4 kHz using electric field data from the double-probe Electric Fields Instrument (EFI) [*Bonnell et al.*, 2008] and magnetic field data from the Search Coil Magnetometer (SCM) [*Roux et al.*, 2008; *LeContel et al.*, 2008]. The resulting wave amplitudes (filter bank data) are included in the survey mode telemetry, covering most orbits with a measurement cadence of four seconds [*Cully et al.*, 2008a]. In the present study filter bank data of wave magnetic field obtained from 1 June 2007 to 1 Feb 2009 for all 5 probes are analyzed to obtain the global distribution of chorus emissions over the radial range between 5 and 10 R_e at magnetic latitudes less than 25°. During this period, the alignment of the apogees of the 5 THEMIS probes gradually changed to provide excellent coverage over all MLT.

[6] The global distribution of the equatorial electron cyclotron frequencies (inferred from the background mag-

[1]Department of Atmospheric and Oceanic Sciences, University of California, Los Angeles, California, USA.
[2]IGPP, University of California, Los Angeles, California, USA.
[3]Swedish Institute of Space Physics, Uppsala, Sweden.
[4]Centre d'étude des Environnements Terrestre et Planétaires, Vélizy, France.
[5]Institut für Geophysik und extraterrestrische Physik, Technischen Universität Braunschweig, Braunschweig, Germany.
[6]Space Research Institute, Austrian Academy of Sciences, Graz, Austria.

0094-8276/09/2009GL037595$05.00

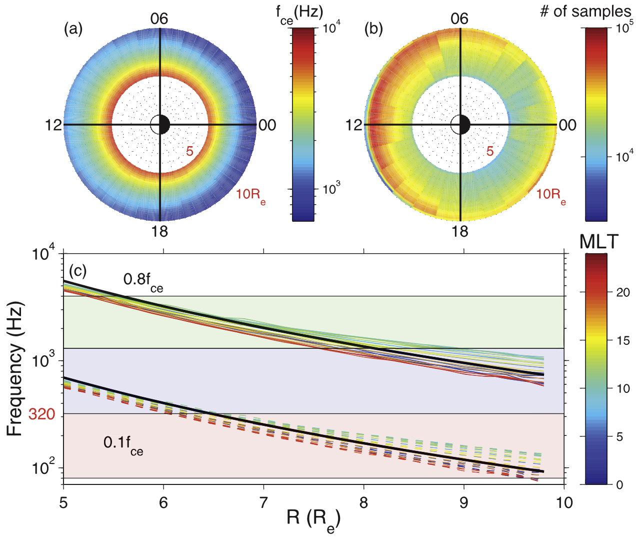

Figure 1. (a) Spatial distribution of the mean value of equatorial electron cyclotron frequency (Hz) and (b) the number of data samples in each corresponding bin between L of 5 and 10 at all MLT. (c) The range of values of typical chorus emissions (0.1 f_{ce} (dashed lines) and 0.8 f_{ce} (solid lines)) as a function of radial distance at the magnetic equator for all MLT represented by different colors. The two bold black lines indicate 0.8 f_{ce} and 0.1 f_{ce} obtained from a pure dipole magnetic field model. The three colored shaded regions ((top) 1390–4000 Hz, (middle) 320–904 Hz, (bottom) 80–227 Hz) represent the top three frequency ranges covered by filter bank data.

netic field data measured from the THEMIS Flux-Gate Magnetometer (FGM) [*Auster et al.*, 2008]), which control the frequency band of chorus, is shown in Figure 1a. Filter bank wave data obtained over the L range between 5 and 10 are consigned to bins with size 0.2 R_e × 1 MLT, and the corresponding number of samples in each bin is shown in Figure 1b. Figure 1c shows the typical frequency range of chorus, between 0.1 f_{ce} (dashed lines) and 0.8 f_{ce} (solid lines), as a function of radial distance, and different MLT is indicated by lines with various colors. The expected dayside compression and nightside stretching of magnetic field lines are clearly evident at the large L-shell. The three colored shaded regions represent the top three frequency ranges covered by filter bank data. For each wave sample, simultaneous equatorial electron cyclotron frequency is used to select the appropriate filter bank data to capture the main power of chorus (e.g., if 0.1 f_{ce} is larger than 320 Hz, chorus is assumed to be confined to the top two filter bank bands; if 0.1 f_{ce} is smaller than 320 Hz, chorus is assumed to occur in the second and third bands). To ensure coverage over the entire band where chorus may occur, data with simultaneous equatorial electron cyclotron frequency larger than 10 kHz or smaller than 800 Hz are excluded from the analysis.

3. Global Distribution of Chorus for Different Magnetic Activity

[7] The dependence of chorus wave intensity on the magnetic activity index AE is first investigated to allow comparison with statistical results from CRRES [*Meredith et al.*, 2003; *Bortnik et al.*, 2007]. THEMIS wave magnetic field amplitudes from filter bank data are first binned as a function of L in steps of 0.2 L and MLT with the interval of 1 hour. Data taken at different magnetic latitudes are mapped to the magnetic equator in Solar Magnetic coordinates using the Tsyganenko 96 magnetic field model [*Tsyganenko and Stern*, 1996] and assigned to the radial distance from the center of the Earth to the equatorial crossing point using the ONERA-DESP library V4.2. The average Root Mean Square (RMS) chorus amplitudes and the number of samples in each bin are shown as a function of L and MLT for three different levels of AE* (the mean value of AE over the previous 1 hour). Figure 2a shows RMS wave magnetic field amplitude in the near–equatorial region ($|MLAT| < 10°$) and Figure 2c shows wave magnetic field in the mid-latitude region ($10° \leq |MLAT| < 25°$). The smaller plots (Figures 2b and 2d) below represent the number of samples in each bin. In the near–equatorial region, chorus intensity on the nightside (up to $L \sim 8$) depends strongly on AE* with much stronger intensity during higher geomagnetic activity. However, around noon, wave intensity is less dependent on AE* and moderate chorus is present even during quiet times (AE* < 100 nT). Note that due to the level of instrumental noise on the top band (1390–4000 Hz) in the 6-band filter bank data, a lower limit of ~3 pT is present all the time, which results in the lowest value of 4 pT in the colorbar. Interestingly, strong nightside chorus is confined to $L \leq 8$, while strong dayside chorus can extend to higher L-shells, consistent with *Tsurutani and Smith* [1977]. In the mid-latitude region, nightside chorus is very weak even during strong magnetic activity (AE* > 300 nT), while strong dayside chorus can be present up to at least $L \sim 10$, peaking around $L \sim 8$, consistent with *Santolik et al.* [2005]. Our new statistical survey is consistent with the previous statistical analysis of *Meredith et al.* [2003] in the region of overlap between the THEMIS and CRRES spacecraft ($5 \leq L \leq 7$). However, the THEMIS data provides compelling new evidence for the persistent presence of chorus on the dayside, during moderate and even weak geomagnetic activity. Such waves are most intense near $L \sim 8$, a region not well sampled by CRRES, both near the equator and in the mid-latitude region. Note that the wave amplitudes from the filter bank data are averaged over four seconds, and the instantaneous amplitudes can greatly exceed these four-second averages, as demonstrated by *Cully et al.* [2008b].

4. Global Occurrence of Chorus Waves Categorized by Different Levels of Wave Amplitude

[8] To evaluate the global occurrence rate of chorus, the wave magnetic field data is first sorted into different levels of wave magnetic field amplitudes (moderate: 10 pT $\leq B_w <$ 30 pT, strong: 30 pT $\leq B_w \leq$ 100 pT, and extremely strong: $B_w >$ 100 pT). The occurrence rate is defined as the ratio of the number of data samples, whose wave amplitude falls in the designated wave amplitude level, to the total number of samples in each bin. Figure 3 shows the occurrence rate (%) of different levels of wave amplitudes in the near-equatorial region ($|MLAT| < 10°$) (Figure 3a) and mid-latitude region

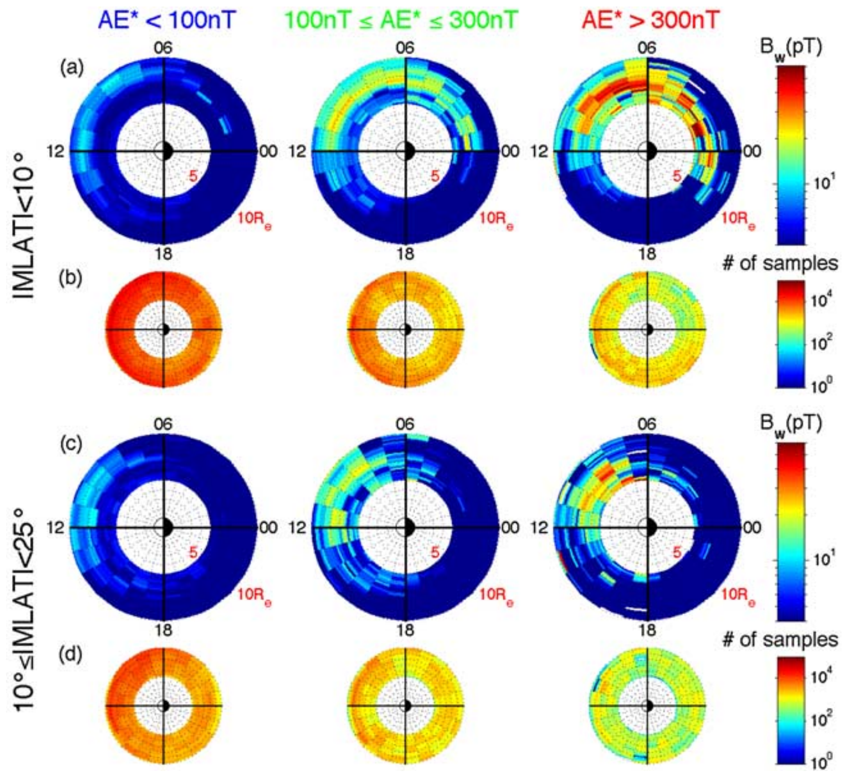

Figure 2. Global distribution of chorus observed at the *L*-shells between 5 and 10 categorized by different AE* in the (a and b) near equatorial (|MLAT| < 10°) and (c and d) mid-latitude regions (10° ≤ |MLAT| < 25°). The larger plots (Figures 1a and 1c) show RMS chorus wave amplitudes (pT) and the smaller plots (Figures 1b and 1d) indicate the number of samples in each bin.

(10° ≤ |MLAT| < 25°) (Figure 3b). In the near-equatorial region, the occurrence rate of both moderate (column 1) and strong (column 2) chorus is larger on the dayside than that on the nightside, and this MLT asymmetry is most apparent at larger *L*-shells. However, for the extremely strong (B_w > 100 pT) chorus, which can lead to non-linear scattering [e.g., *Bortnik et al.*, 2008], the occurrence rate tends to be larger in the region between the nightside and the dawnside (with relatively poor statistics due to the much less data points). In the mid-latitude region, the asymmetry of the

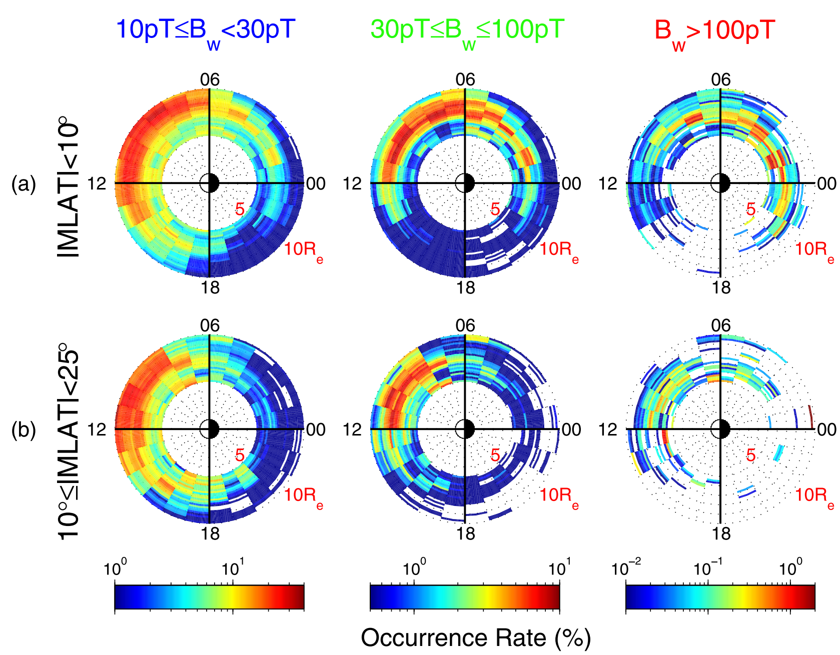

Figure 3. Global distribution of occurrence rate (%) categorized by different levels of wave amplitudes (a) in the near-equatorial region (|MLAT| < 10°) and (b) in the mid-latitude region (10° ≤ |MLAT| < 25°).

occurrence rate of moderate and strong chorus on the dayside and nightside is even more pronounced, with differences of almost an order of magnitude. These interesting features, which have not been reported in previous studies, provide important clues on the source mechanism for dayside and nightside chorus.

5. Summary and Discussion

[9] Filter bank data from THEMIS are used to provide a global picture of chorus wave distribution in the magnetosphere. Our statistical study covers a broader region ($5 \leq L \leq 10$) and shows consistent results in the overlap region ($5 \leq L \leq 7$) with the recent CRRES analysis [*Meredith et al.*, 2003]. Most importantly, the new THEMIS results on the occurrence rates of different levels of chorus amplitudes provide interesting insight into the generation mechanism at relatively higher *L*-shells.

[10] The main results of this study can be summarized as follows.

[11] 1. The RMS amplitudes of chorus are dependent on AE*; wave amplitudes tend to maximize at $L < 7$ on the nightside and $L > 7$ on the pre-noon. However, moderate chorus (>10 pT) is present on the dayside even during quiet times (AE* < 100 nT).

[12] 2. Nightside chorus is stronger near the equator ($|\text{MLAT}| < 10°$) and becomes much weaker at higher latitudes ($|\text{MLAT}| \geq 10°$), while strong dayside chorus can extend to higher magnetic latitude ($|\text{MLAT}| \geq 10°$), consistent with *Tsurutani and Smith* [1977] and *Meredith et al.* [2003].

[13] 3. The occurrence rate of the moderate ($10\ \text{pT} \leq B_w < 30\ \text{pT}$) and strong ($30\ \text{pT} \leq B_w \leq 100\ \text{pT}$) dayside chorus is much larger than that on the nightside in both the near-equatorial region and at mid-latitudes particularly at higher *L*-shells.

[14] Whistler mode instability in the magnetosphere requires the presence of a critical resonant electron flux with sufficient pitch angle anisotropy, and the critical flux is proportional to L^{-4} [*Kennel and Petschek*, 1966]. Based on this concept, the THEMIS results suggest the following scenario for the global excitation of chorus emissions.

[15] a. During geomagnetically inactive times, nightside electrons at larger *L* tend to have a butterfly distribution [*West et al.*, 1973], which is stable to whistler excitation. However, convective injection events can provide a source of anisotropic and enhanced electron flux needed to excite nightside chorus [e.g., *Li et al.*, 2008, 2009]. Therefore, the occurrence of chorus on the nightside is low and only associated with enhanced geomagnetic activity.

[16] b. The persistence of dayside chorus during quiet conditions and the high occurrence of dayside chorus at $L > 7$ could result from the natural enhancement of electron anisotropy in the noon sector [e.g., *West et al.*, 1973]. Wave excitation is favored at higher *L*, where the critical stably trapped flux levels are low. Dayside wave excitation can be further enhanced by solar wind driven compressions and electron injections. Such concepts will be tested in our continuing analysis of dayside chorus events.

[17] **Acknowledgments.** This research was funded by the NSF grant ATM_0802843, NASA Heliophysics Theory Program grant NNX08A035G, NASA NAS5-02099, and German Ministerium für Wirtschaft und Technologie and the Deutsches Zentrum für Luft- und Raumfahrt under grant 50QP0402. The authors thank the ONERA library for providing the tools to obtain the location of the geomagnetic equator as well as the World Data Center for Geomagnetism, Kyoto for providing AE and Dst indices.

References

Anderson, R. R., and K. Maeda (1977), VLF emissions associated with enhanced magnetospheric electrons, *J. Geophys. Res.*, *82*(1), 135–146.
Angelopoulos, V. (2008), The THEMIS mission, *Space Sci. Rev.*, *141*(1–4), 5–34, doi:10.1007/s11214-008-9336-1.
Auster, U., et al. (2008), The THEMIS fluxgate magnetometer, *Space Sci. Rev.*, *141*(1–4), 235–264, doi:10.1007/s11214-008-9365-9.
Bonnell, J. W., et al. (2008), The electric field instrument (EFI) for THEMIS, *Space Sci. Rev.*, *141*(1–4), 303–341, doi:10.1007/s11214-008-9469-2.
Bortnik, J., R. M. Thorne, and N. P. Meredith (2007), Modeling the propagation characteristics of chorus using CRRES suprathermal electron fluxes, *J. Geophys. Res.*, *112*, A08204, doi:10.1029/2006JA012237.
Bortnik, J., R. M. Thorne, and U. S. Inan (2008), Nonlinear interaction of energetic electrons with large amplitude chorus, *Geophys. Res. Lett.*, *35*, L21102, doi:10.1029/2008GL035500.
Cully, C. M., R. E. Ergun, K. Stevens, A. Nammari, and J. Westfall (2008a), The THEMIS digitial fields board, *Space Sci. Rev.*, *141*(1–4), 343–355, doi:10.1007/s11214-008-9417-1.
Cully, C. M., J. W. Bonnell, and R. E. Ergun (2008b), THEMIS observations of long-lived regions of large-amplitude whistler waves in the inner magnetosphere, *Geophys. Res. Lett.*, *35*, L17S16, doi:10.1029/2008GL033643.
Horne, R. B., and R. M. Thorne (1998), Potential waves for relativistic electron scattering and stochastic acceleration during magnetic storms, *Geophys. Res. Lett.*, *25*(15), 3011–3014.
Horne, R. B., and R. M. Thorne (2003), Relativistic electron acceleration and precipitation during resonant interactions with whistler-mode chorus, *Geophys. Res. Lett.*, *30*(10), 1527, doi:10.1029/2003GL016973.
Horne, R. B., R. M. Thorne, S. A. Glauert, J. M. Albert, N. P. Meredith, and R. R. Anderson (2005), Timescale for radiation belt electron acceleration by whistler mode chorus waves, *J. Geophys. Res.*, *110*, A03225, doi:10.1029/2004JA010811.
Kennel, C. F., and H. E. Petschek (1966), Limit on stably trapped particle fluxes, *J. Geophys. Res.*, *71*(1), 1–28.
LeContel, O., et al. (2008), First results of the THEMIS searchcoil magentometers, *Space Sci. Rev.*, *141*(1–4), 509–534, doi:10.1007/s11214-008-9371-y.
LeDocq, M. J., D. A. Gurnett, and G. B. Hospodarsky (1998), Chorus source locations from VLF Poynting flux measurements with the polar spacecraft, *Geophys. Res. Lett.*, *25*(21), 4063–4066.
Li, W., Y. Y. Shprits, and R. M. Thorne (2007), Dynamic evolution of energetic outer zone electrons due to wave-particle interactions during storms, *J. Geophys. Res.*, *112*, A10220, doi:10.1029/2007JA012368.
Li, W., R. M. Thorne, N. P. Meredith, R. B. Horne, J. Bortnik, Y. Y. Shprits, and B. Ni (2008), Evaluation of whistler mode chorus amplification during an injection event observed on CRRES, *J. Geophys. Res.*, *113*, A09210, doi:10.1029/2008JA013129.
Li, W., R. M. Thorne, V. Angelopoulos, J. W. Bonnell, J. P. McFadden, C. W. Carlson, O. LeContel, A. Roux, K. H. Glassmeier, and H. U. Auster (2009), Evaluation of whistler-mode chorus intensification on the nightside during an injection event observed on the THEMIS spacecraft, *J. Geophys. Res.*, *114*, A00C14, doi:10.1029/2008JA013554.
Lorentzen, K. R., J. B. Blake, U. S. Inan, and J. Bortnik (2001), Observations of relativistic electron microbursts in association with VLF chorus, *J. Geophys. Res.*, *106*(A4), 6017–6027.
Meredith, N. P., R. B. Horne, and R. R. Anderson (2001), Substorm dependence of chorus amplitudes: Implications for the acceleration of electrons to relativistic energies, *J. Geophys. Res.*, *106*(A7), 13,165–13,178.
Meredith, N. P., R. B. Horne, R. H. A. Iles, R. M. Thorne, D. Heynderickx, and R. R. Anderson (2002), Outer zone relativistic electron acceleration associated with substorm-enhanced whistler mode chorus, *J. Geophys. Res.*, *107*(A7), 1144, doi:10.1029/2001JA900146.
Meredith, N. P., R. B. Horne, R. M. Thorne, and R. R. Anderson (2003), Favored regions for chorus-driven electron acceleration to relativistic energies in the Earth's outer radiation belt, *Geophys. Res. Lett.*, *30*(16), 1871, doi:10.1029/2003GL017698.
O'Brien, T. P., M. D. Looper, and J. B. Blake (2004), Quantification of relativistic electron microburst losses during the GEM storms, *Geophys. Res. Lett.*, *31*, L04802, doi:10.1029/2003GL018621.
Parrot, M., and C. A. Gaye (1994), A statistical survey of ELF waves in a geostationary orbit, *Geophys. Res. Lett.*, *21*(23), 2463–2466.
Roux, A., O. LeContel, C. Coillot, A. Bouabdellah, B. de la Porte, D. Alison, S. Ruocco, and M. C. Vassal (2008), The search coil magentometer for THEMIS, *Space Sci. Rev.*, *141*(1–4), 265–275, doi:10.1007/s11214-008-9455-8.

Santolík, O., D. A. Gurnett, J. S. Pickett, M. Parrot, and N. Cornilleau-Wehrlin (2003), Spatio-temporal structure of storm-time chorus, *J. Geophys. Res.*, *108*(A7), 1278, doi:10.1029/2002JA009791.

Santolik, O., E. Macusova, K. H. Yearby, N. Cornilleau-Wehrlin, and H. StC. K. Alleyne (2005), Radial variation of whistler-mode chorus: First results from the STAFF/DWP instrument onboard the Double Star TC 1 spacecraft, *Ann. Geophys.*, *23*, 2937–2942.

Shprits, Y. Y., R. M. Thorne, R. B. Horne, S. A. Glauert, M. Cartwright, C. T. Russell, D. N. Baker, and S. G. Kanekal (2006), Acceleration mechanism responsible for the formation of the new radiation belt during the 2003 Halloween solar storm, *Geophys. Res. Lett.*, *33*, L05104, doi:10.1029/2005GL024256.

Summers, D., R. M. Thorne, and F. Xiao (1998), Relativistic theory of wave-particle resonant diffusion with application to electron acceleration in the magnetosphere, *J. Geophys. Res.*, *103*(A9), 20,487–20,500.

Summers, D., C. Ma, N. P. Meredith, R. B. Horne, R. M. Thorne, D. Heynderickx, and R. R. Anderson (2002), Model of the energization of outer-zone electrons by whistler-mode chorus during the October 9, 1990 geomagnetic storm, *Geophys. Res. Lett.*, *29*(24), 2174, doi:10.1029/2002GL016039.

Summers, D., B. Ni, and N. P. Meredith (2007), Timescales for radiation belt electron acceleration and loss due to resonant wave-particle interactions: 1. Theory, *J. Geophys. Res.*, *112*, A04206, doi:10.1029/2006JA011801.

Thorne, R. M., T. P. O'Brien, Y. Y. Shprits, D. Summers, and R. B. Horne (2005), Timescale for MeV electron microburst loss during geomagnetic storms, *J. Geophys. Res.*, *110*, A09202, doi:10.1029/2004JA010882.

Thorne, R. M., Y. Y. Shprits, N. P. Meredith, R. B. Horne, W. Li, and L. R. Lyons (2007), Refilling of the slot region between the inner and outer electron radiation belts during geomagnetic storms, *J. Geophys. Res.*, *112*, A06203, doi:10.1029/2006JA012176.

Tsurutani, B. T., and E. J. Smith (1974), Postmidnight chorus: A substorm phenomenon, *J. Geophys. Res.*, *79*(1), 118–127.

Tsurutani, B. T., and E. J. Smith (1977), Two types of magnetospheric ELF chorus and their substorm dependences, *J. Geophys. Res.*, *82*(32), 5112–5128.

Tsyganenko, N. A., and D. P. Stern (1996), Modeling the global magnetic field of the large-scale Birkeland current systems, *J. Geophys. Res.*, *101*(A12), 27,187–27,198.

West, H. I., Jr., R. M. Buck, and J. R. Walton (1973), Electron pitch angle distributions throughout the magnetosphere as observed on Ogo 5, *J. Geophys. Res.*, *78*(7), 1064–1081.

V. Angelopoulos, IGPP, University of California, CA 90095-1567, USA. (vassilis@ucla.edu)

U. Auster, Institut für Geophysik und extraterrestrische Physik, Technischen Universität Braunschweig, Mendelssohnstrasse 3, D-38106 Braunschweig, Germany. (uli.auster@tu-braunschweig.de)

J. Bortnik, W. Li, B. Ni, and R. M. Thorne, Department of Atmospheric and Oceanic Sciences, University of California, 405 Hilgard Avenue, Los Angeles, CA 90095-1565, USA. (jbortnik@gmail.com; moonli@atmos.ucla.edu; bbni@atmos.ucla.edu; rmt@atmos.ucla.edu)

C. M. Cully, Swedish Institute of Space Physics, Box 537, SE-751 21 Uppsala, Sweden. (chris@irfu.se)

O. LeContel and A. Roux, Centre d'étude des Environnements Terrestre et Planétaires, 10-12 Avenue de l'Europe, F-78140 Vélizy, France. (olivier.lecontel@cetp.ipsl.fr; alain.roux@cetp.ipsl.fr)

W. Magnes, Space Research Institute, Austrian Academy of Sciences, Schmiedlstrasse 6, A-8042 Graz, Austria. (werner.magnes@oeaw.ac.at)